

Modelling of silicon condenser microphones

A.G.H. van der Donk*, P.R. Scheeper**, W. Olthuis and P. Bergveld

MESA Research Institute, University of Twente, PO Box 217, 7500 AE Enschede (Netherlands)

(Received January 12, 1993, in revised form November 19, 1993, accepted December 3, 1993)

Abstract

Several models concerning the sensitivity of capacitive pressure sensors have been presented in the past. Modelling of condenser microphones, which can be considered to be a special type of capacitive pressure sensor, usually requires a more complicated analysis of the sensitivity, because they have a strong electric field in the air gap. It is found that the mechanical sensitivity of condenser microphones with a circular diaphragm, either with a large initial tension or without any initial tension, increases with increasing bias voltage (and the corresponding static deflection), whereas the mechanical sensitivity of other capacitive pressure sensors does not depend on the static deflection. It is also found that the mechanical sensitivity increases with increasing input capacitance of a preamplifier. In addition, the open-circuit electrical sensitivity and, consequently, the total sensitivity too, also increases with increasing bias voltage (or static deflection). However, the maximum allowable sound pressure at which the diaphragm collapses, an effect that has to be taken into account, decreases with increasing static deflection in most cases, ultimately resulting in an optimum value for the bias voltage. The model for microphones with a circular highly tensioned diaphragm has been verified successfully for two microphone types.

1. Introduction

During the last decade modelling has become very important for designing a condenser microphone or pressure sensor with a desired sensitivity. Several papers concerning the modelling of microphone or pressure sensor diaphragms were presented in the past [1–10, 16]. Warren *et al* [1, 2] calculated numerically the relation between the static deflection of the diaphragm and the electrostatic force between the diaphragm and backplate for diaphragms with a large initial tensile stress, but they did not analyse the sensitivity of the microphone for audio frequencies. In a later paper they also considered the sensitivity of microphones, but they did not analyse electrostatic effects caused by the presence of a bias voltage of an electret, which is generally needed for condenser microphones.

Other authors [4–9] considered only deflections of diaphragms due to a homogeneous pressure. Ko *et al* [5] and Voorthuyzen *et al* [10] described the effect of reducing the electrode area of the diaphragm on the performance of the sensor, which results in an increase in the sensitivity.

In this paper only static and quasi-static diaphragm deflections will be considered. Other dynamic considerations, such as bandwidth and resonance frequency, are not presented here, because these parameters are investigated extensively in other papers [11–15] and can easily be manipulated by changing the intensity of the backplate perforation.

Because circular diaphragms can more easily be described than square diaphragms, the model presented in this paper will only concern circular diaphragms. A comparison between square diaphragms and circular diaphragms shows that the static deflection of a circular diaphragm due to a homogeneous load is maximally 20% larger than the deflection of a square diaphragm with the same load, if both diaphragms have the same area [16].

Analytical expressions will be derived for the static deflection of circular diaphragms due to a homogeneous load and due to an electrostatic force, which turns out to be inhomogeneous. Equations will be given for the sensitivity of the microphone as well as the maximum allowable sound pressure. Both stress-free diaphragms and diaphragms with a large initial tensile stress will be considered, because only in these situations does a small temperature dependence of the sensitivity of diaphragms occur [14, 17].

Timoshenko and Woinowski-Krieger [18] have derived a relation between a homogeneous load on a

*Present address: Texas Instruments Holland B.V., PO Box 43, 7600 AA Almelo, Netherlands.

**Present address: Bruel & Kjaer, Skodsborgvej 307, DK 2850 Nærum, Denmark.

stress-free plate and the resulting deflection. In Section 2 a theoretical relation is derived between the load and the deflection of a plate with a large initial stress using the energy method, which is similar to the method used in ref. 18. By means of an energy calculation it is also possible to derive relations between the deflection and a non-homogeneous (electrostatic) load. By using this method it is possible to calculate the d.c. voltage between the two condenser plates necessary to obtain a desired centre deflection of the diaphragm. This calculation is presented in Section 3.

The mechanical sensitivity of the microphone is discussed in Section 4, the electrical in Section 5 and the total sensitivity in Section 6.

Furthermore, some general criteria concerning the maximum allowable sound pressure at which the diaphragm collapses into the direction of the backplate will be discussed in Section 7.

In Section 8 some experimental results are presented to verify some of the expressions presented in this paper.

2. Static deflection of a diaphragm due to a homogeneous load

In this Section a relation between a homogeneous load and the corresponding deflection will be derived for both stress-free diaphragms and diaphragms with a large initial stress. The calculations will be carried out using the energy method, which has been described by Timoshenko and Woinowski-Krieger [18]. The results will be compared with the solutions of a numerical procedure presented by Voorthuyzen *et al.* [8], which in addition calculates the deflection of diaphragms with a small initial stress.

Note that a distinction will be made between a diaphragm, a membrane and a thin plate. The word diaphragm is used as a general expression, including membranes and plates. A thin plate is a diaphragm without any initial stress, having a deflection that is only determined by the flexural rigidity of the diaphragm, if it is loaded. A membrane is a diaphragm with a large initial stress, having a deflection that is mainly determined by that stress, when loaded.

2.1 Deflection of a stress-free diaphragm

Timoshenko and Woinowski-Krieger [18] derived an expression for the energy of a circular thin plate for a given deflection w_0 at the centre. It consists of two components, the bending energy V_0 and the strain energy V_1 . An incremental centre displacement δw_0 of the plate causes an increase in the energy, resulting in a reaction force. This energy increase δW_r is equal to [18]

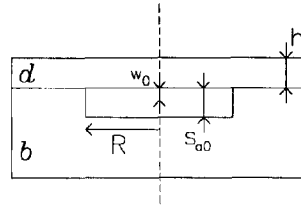


Fig. 1 Cross-sectional view of condenser microphone, with b the backplate, d the diaphragm, s_{a0} the thickness and R the radius of the air gap, and h the thickness of the diaphragm. The centre diaphragm deflection is indicated by w_0 .

$$\begin{aligned} \delta W_r &= \frac{d(V_0 + V_1)}{dw_0} \delta w_0 \\ &= \frac{\pi}{3} \frac{E_d h^3}{0.171 R^2} \left(w_0 + 0.488 \frac{w_0^3}{h^2} \right) \delta w_0 \end{aligned} \quad (1)$$

where E_d is Young's modulus, h the thickness and R the radius of the thin plate. A schematic view of the microphone, which illustrates the deflection w_0 of the diaphragm, is shown in Fig. 1.

It is shown [8, 20] that the deflection $w(r)$ of the thin plate has a fourth-order polynomial curvature

$$w(r) = w_0 \left[1 - \left(\frac{r}{R} \right)^2 \right]^2 \quad (2)$$

with w_0 the centre deflection and r the distance to the centre.

For a homogeneous load (a pressure P) the energy δW necessary to increase the centre deflection with an incremental displacement δw_0 is [18]

$$\delta W = \int_0^R P \delta w(r) 2\pi r dr = \frac{1}{3} \pi R^2 P \delta w_0 \quad (3)$$

By taking $\delta W = \delta W_r$, a relation can be found between a homogeneous load P and the centre deflection of the circular plate

$$P = \frac{E_d h^3}{0.171 R^4} \left(w_0 + 0.488 \frac{w_0^3}{h^2} \right) \quad (4)$$

Note that the third-order term can be neglected if $0.488(w_0/h)^2 \ll 1$, or $w_0/h \ll 1.4$. If $w_0/h < 0.45$, the relative contribution of the third-order term is maximally 10%.

2.2 Deflection of a diaphragm with a large initial tensile stress

Similarly, the energy of a circular diaphragm with a large initial tensile stress, usually called a membrane, can be calculated. Because the strain energy V_1 is dominating, the energy V_0 due to bending can be neglected. The initial stress is considered to be homogeneous and isotropic.

The curvature of the membrane is parabolic [8]

$$w(r) = w_0 \left[1 - \left(\frac{r}{R} \right)^2 \right] \quad (5)$$

If a third-order polynomial is taken for the radial displacement, it can be derived that the energy increase due to an incremental centre displacement δw_0 is [20]

$$\delta W_r = \left(2\pi\sigma_d h w_0 + 1.595\pi E_d h \frac{w_0^3}{R^2} \right) \delta w_0 \quad (6)$$

similarly to the considerations concerning thin plates as described in ref 18. In eqn (6) σ_d is the initial diaphragm stress in Pa.

For a homogeneous load (a pressure P) the energy necessary to perform this incremental displacement δw_0 is [20]

$$\delta W = \int_0^R P \delta w(r) 2\pi r dr = \frac{1}{2} \pi R^2 P \delta w_0 \quad (7)$$

By taking $\delta W = \delta W_r$, a relation can be found between a homogeneous load and the centre deflection of the circular membrane

$$P = 4\sigma_d \frac{h}{R^2} w_0 + 3.19E_d \frac{h}{R^4} w_0^3 \quad (8)$$

Note that the contribution of the third-order term is less than 10% if

$$\frac{\sigma_d}{E_d} \left(\frac{R}{w_0} \right)^2 > \frac{31.9}{4}$$

or

$$\frac{\sigma_d}{E_d} \left(\frac{R}{h} \right)^2 > 7.98 \left(\frac{w_0}{h} \right)^2$$

2.3 Evaluation of the two models

If the third-order terms are neglected (small deflections), expressions (4) and (8) are equal if $(R/h)^2 \sigma_d / E_d = 1.46$. For $(R/h)^2 \sigma_d / E_d \gg 1.46$, eqn (8) is valid. For $(R/h)^2 \sigma_d / E_d \ll 1.46$, eqn (4) should be used.

By using the numerical algorithm of Voorthuyzen *et al* [8], which also calculates the deflection as a function of the homogeneous load for diaphragms with a small initial stress, it is possible to evaluate both models. In Fig 2 the relative difference between both models and the numerical model of Voorthuyzen is shown as a function of $(R/h)^2 \sigma_d / E_d$.

As can be seen from this Figure, the difference between eqn (4) and the numerical model is smaller than 10% for values of $(R/h)^2 \sigma_d / E_d$ smaller than 0.125. The difference between eqn (8) and the numerical model is smaller than 10% for $(R/h)^2 \sigma_d / E_d > 50$.

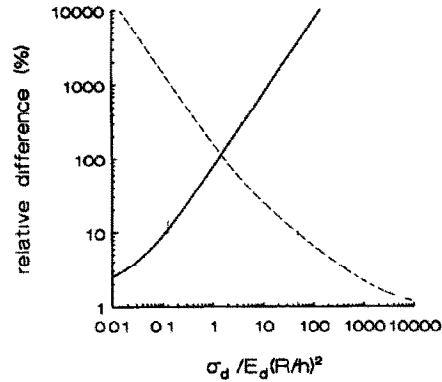


Fig 2 Relative difference between the model for stress-free diaphragms according to eqn (4) and the numerical model of Voorthuyzen *et al* [8] (solid line), and the relative difference between the model for diaphragms with large initial stress according to eqn (8) and the numerical model of Voorthuyzen *et al* [8] (dashed line)

Note that if $(R/h)^2 \sigma_d / E_d > 50$, the relative contribution of the third-order term in eqn (8) is less than 10% for $w_0/h < (50/7.98)^{1/2}$ or $w_0/h < 2.5$. Therefore, the third-order term can be neglected in most cases.

From these considerations, as mentioned previously, it can be concluded that the inaccuracy of eqn (4) is less than 10% for $(R/h)^2 \sigma_d / E_d < 0.125$, and for $(R/h)^2 \sigma_d / E_d > 50$ the inaccuracy of eqn (8) is less than 10%.

3. Static deflection of a diaphragm due to an electrostatic force

Condenser microphones usually need a d.c. electric field in the air gap to obtain an a.c. output signal if the microphone capacitance changes due to an acoustic pressure [1, 2, 16]. This d.c. field can be realized by means of an external d.c. voltage supply or by using an electret. In both cases the force caused by the d.c. field is not homogeneous, like the external load as described in the previous Section. The electrostatic attractive force per unit area, P_e , caused by the electric field, depends on r according to

$$P_e(r) = \frac{\epsilon_0}{2} \left(\frac{V}{s_a - w(r)} \right)^2 \quad (9)$$

with ϵ_0 the permittivity of vacuum, s_a the effective thickness of the air gap and V the bias voltage. In eqn (9) s_a is the sum of the physical air-gap thickness, s_{a0} , and the thickness of the diaphragm multiplied by the ratio of the relative permittivity ϵ_a of air to the relative permittivity ϵ_m of the diaphragm material. Because the value of ϵ_a can be considered to be equal to one, s_a can be expressed as

$$s_a = s_{a0} + \frac{h}{\epsilon_m} \quad (10)$$

By considering an incremental centre displacement δw_0 , as in the previous Sections, the electrostatic energy δW_e needed to perform this displacement can be calculated

$$\begin{aligned} \delta W_e &= \int_0^R P_e \delta w(r) 2\pi r dr \\ &= \pi \frac{\epsilon_0}{2} V^2 \int_0^R \left(\frac{1}{s_a - w(r)} \right)^2 \delta w(r) 2r dr \end{aligned} \quad (11)$$

Note that $\delta w(r)$ is described by eqn (3) if the diaphragm has no initial stress and by eqn (7) if the diaphragm has an initial tensile stress σ_d . Both cases will be treated in the next Section

3.1 Deflection of a stress-free diaphragm

By using eqns (2) and (3) in eqn (11), δW_e can be expressed as

$$\begin{aligned} \delta W_e &= \frac{\pi R^2 \epsilon_0 V^2}{4w_0} \delta w_0 \\ &\times \left[\frac{1}{s_a - w_0} - \frac{1}{2(s_a w_0)^{1/2}} \ln \left(\frac{s_a^{1/2} + w_0^{1/2}}{s_a^{1/2} - w_0^{1/2}} \right) \right] \end{aligned} \quad (12)$$

Because the force per unit area P_e is not homogeneous, effective forces \bar{P} , \bar{P}_r and \bar{P}_e per unit area will be introduced, which can be calculated from the energies δW , δW_r and δW_e , respectively, by dividing them by $\pi R^2 \delta w_0$. The effective forces per unit area \bar{P} and \bar{P}_e are only equal to the real (homogeneous) forces per unit area P and P_e when the diaphragm is flat and has a piston-like movement

With the introduction of the effective forces per unit area, eqns (1), (3) and (12) become, respectively,

$$\bar{P}_r = \frac{1}{3} \frac{E_d}{0.171 R^4} \left(\frac{w_0}{h} + 0.488 \frac{w_0^3}{h^3} \right) \quad (13)$$

$$\bar{P} = \frac{1}{3} P \quad (14)$$

and

$$\begin{aligned} \bar{P}_e &= \frac{\epsilon_0}{4w_0/s_a} \left(\frac{V}{s_a} \right)^2 \\ &\times \left[\frac{1}{1 - w_0/s_a} - \frac{1}{2(w_0/s_a)^{1/2}} \ln \left[\frac{1 + (w_0/s_a)^{1/2}}{1 - (w_0/s_a)^{1/2}} \right] \right] \end{aligned} \quad (15)$$

By dividing eqns (13) and (15) by E_d , dimensionless equations are obtained

$$\frac{\bar{P}_r}{E_d} = \frac{1}{0.513} \frac{1}{(R/s_a)^4} \left[\frac{w_0}{s_a} \left(\frac{h}{s_a} \right)^3 + 0.488 \left(\frac{w_0}{s_a} \right)^3 \frac{h}{s_a} \right] \quad (16)$$

and

$$\begin{aligned} \frac{\bar{P}_e}{E_d} &= \frac{1}{2w_0/s_a} \frac{\epsilon_0 (V/s_a)^2}{2E_d} \\ &\times \left\{ \frac{1}{1 - w_0/s_a} - \frac{1}{2(w_0/s_a)^{1/2}} \ln \left[\frac{1 + (w_0/s_a)^{1/2}}{1 - (w_0/s_a)^{1/2}} \right] \right\} \end{aligned} \quad (17)$$

Note that $(\epsilon_0/2)(V/s_a)^2$ represents the normalized electrostatic attractive force per unit area for complete rigid parallel plates

If the external pressure P is absent, \bar{P}_r/E_d and \bar{P}_e/E_d can be plotted as a function of the dimensionless centre deflection, w_0/s_a , if the dimensionless parameters h/s_a , R/s_a and $\epsilon_0(V/s_a)^2/(2E_d)$ have been chosen. In Fig 3 both normalized forces per unit area are shown as a function of w_0/s_a for $h/s_a=1$, $R/s_a=1000$ and $\epsilon_0(V/s_a)^2/(2E_d)=1 \times 10^{-12}$. The values of these parameters are based on values for microphones with a silicon nitride diaphragm, realized by Scheeper *et al* [19], with $h=1 \mu\text{m}$, $s_a=1 \mu\text{m}$, $R=1 \text{mm}$ and $V=0.185 \text{V}$, where $E_d=1.5 \times 10^{11} \text{Pa}$ has been assumed

As can be seen, there are two values of w_0/s_a for which the effective forces per unit area are equal. The dimensionless net attractive force per unit area, $(\bar{P}_e - \bar{P}_r)/E_d$, which is also shown in Fig 3, is equal to zero for these two values. The low value is the stable working point, because the derivative of the net function is negative. The high value is not stable and the net function has a positive derivative at this value.

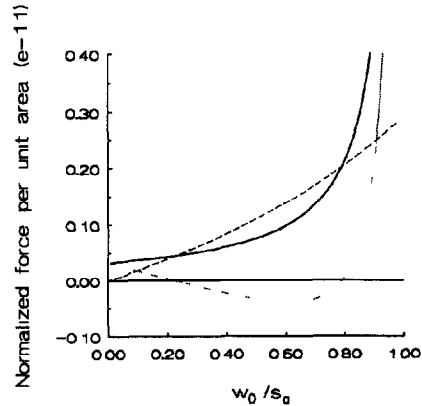


Fig 3 Normalized electrostatic force \bar{P}_e/E_d (—), reaction force \bar{P}_r/E_d (---) and their difference $(\bar{P}_e - \bar{P}_r)/E_d$ (- · -) per unit area as a function of the normalized centre deflection w_0/s_a , with $h/s_a=1$, $R/s_a=1000$ and $\epsilon_0(V/s_a)^2/(2E_d)=1 \times 10^{-12}$. Diaphragm without initial stress

If $\epsilon_0(V/s_a)^2/(2E_d)$ increases, the curve of the dimensionless electrostatic force shifts upwards, and the distance between the two zero-values of the net function decreases. For $\epsilon_0(V/s_a)^2/(2E_d)=1.45 \times 10^{-12}$, there is only one zero-value. For larger values, \bar{P}_e/E_d is always larger than \bar{P}_r/E_d and the diaphragm will stick to the backplate. Therefore, it can be concluded that the value of $\epsilon_0(V/s_a)^2/(2E_d)$ cannot be chosen infinitely large.

For lower values of $\epsilon_0(V/s_a)^2/(2E_d)$, it is possible to calculate the voltage to be applied for a certain deflection w_0 by equating eqn (13) with eqn (15). Consequently, a relation is obtained between the static deflection w_0 and the corresponding voltage for given values of E_d , h , R and s_a .

$$V^2 = \frac{\frac{1}{3} s_a^2 \frac{E_d}{0.171 R^4} \left(\frac{w_0}{h} + 0.488 \frac{w_0^3}{h^3} \right)}{\frac{\epsilon_0}{4w_0/s_a} \left\{ \frac{1}{1-w_0/s_a} - \frac{1}{2(w_0/s_a)^{1/2}} \ln \left[\frac{1+(w_0/s_a)^{1/2}}{1-(w_0/s_a)^{1/2}} \right] \right\}} \quad (18)$$

For each value of V , two corresponding values of the static deflection w_0 can be found, of which the lower value determines the stable working point.

3.2 Deflection of a diaphragm with a large initial tensile stress

By substituting eqns (5) and (7) in eqn (11), δW_c can be expressed as

$$\delta W_c = \frac{\pi R^2 \epsilon_0 V^2 \delta w_0}{2w_0} \left[\frac{1}{s_a - w_0} + \frac{1}{w_0} \ln \left(1 - \frac{w_0}{s_a} \right) \right] \quad (19)$$

By dividing expressions (6), (7) and (19) by δw_0 and πR^2 , the effective forces per unit area \bar{P}_r , \bar{P} and \bar{P}_e are obtained

$$\bar{P}_r = 2 \frac{\sigma_d h w_0}{R^2} + 1.595 E_d h \frac{w_0^3}{R^4} \quad (20)$$

$$\bar{P} = \frac{1}{2} P \quad (21)$$

and

$$\bar{P}_e = \frac{\epsilon_0 V^2}{2w_0} \left[\frac{1}{s_a - w_0} + \frac{1}{w_0} \ln \left(1 - \frac{w_0}{s_a} \right) \right] \quad (22)$$

Equations (20) and (22) become, in dimensionless form,

$$\frac{\bar{P}_r}{\sigma_d} = \frac{1}{(R/s_a)^4} \left[2 \left(\frac{R}{s_a} \right)^2 \frac{h}{s_a} \frac{w_0}{s_a} + 1.595 \frac{E_d}{\sigma_d} \frac{h}{s_a} \left(\frac{w_0}{s_a} \right)^3 \right] \quad (23)$$

and

$$\frac{\bar{P}_e}{\sigma_d} = \frac{1}{w_0/s_a} \frac{\epsilon_0 (V/s_a)^2}{2\sigma_d}$$

$$\times \left[\frac{1}{1-w_0/s_a} + \frac{1}{w_0/s_a} \ln \left(1 - \frac{w_0}{s_a} \right) \right] \quad (24)$$

Note that in eqns (23) and (24) the force per unit area has been divided by the stress σ_d instead of the Young's modulus E_d , because E_d has negligible influence on the behaviour of the membrane, as shown in the previous Section.

In Fig 4, \bar{P}_r/σ_d , \bar{P}_e/σ_d and the net force per unit area, $(\bar{P}_e - \bar{P}_r)/\sigma_d$, are plotted as a function of the dimensionless centre deflection, w_0/s_a , for $h/s_a=1$, $R/s_a=1000$, $E_d/\sigma_d=1 \times 10^3$ and $\epsilon_0(V/s_a)^2/(2\sigma_d)=4 \times 10^{-7}$, similarly to Fig 3. Again, the values are based on the practical parameters of microphones realized by Scheeper *et al* [19], with $\sigma_d=1.5 \times 10^8$ Pa and $V=3.7$ V.

For these microphones, the value of $\epsilon_0(V/s_a)^2/(2\sigma_d)$ should be chosen not larger than 8.3×10^{-7} to prevent sticking of the membrane to the backplate.

By equating eqns (20) and (22), the relation between the deflection w_0 and the corresponding bias voltage V is obtained

$$V^2 = \frac{2 \frac{\sigma_d h w_0}{R^2} + 1.595 E_d h \frac{w_0^3}{R^4}}{\frac{\epsilon_0}{2w_0} \left[\frac{1}{s_a - w_0} + \frac{1}{w_0} \ln \left(1 - \frac{w_0}{s_a} \right) \right]} \quad (25)$$

Note that the curves in Fig 4 have the same shape as the curves in Fig 3. However, the dimensionless forces per unit area in Fig 4 are approximately 10^6 times larger than in Fig 3. This is partly due to the fact that in Fig 3 the forces per unit area are normalized to the Young's modulus E_d , whereas in Fig 4 they are normalized to the initial stress σ_d . This introduces a difference of a factor of 1000 in these Figures. The

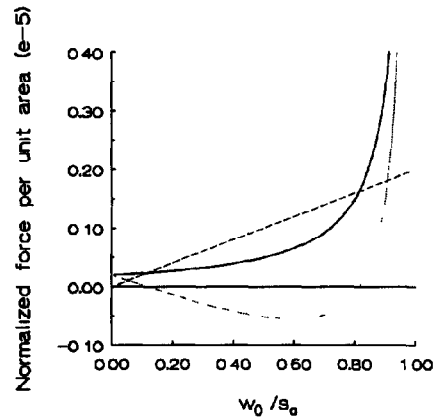


Fig 4 Normalized electrostatic force \bar{P}_e/σ_d (—), reaction force \bar{P}_r/σ_d (---) and their difference $(\bar{P}_e - \bar{P}_r)/\sigma_d$ (· · ·) per unit area as a function of the normalized centre deflection w_0/s_a , with $h/s_a=1$, $R/s_a=1000$, $\epsilon_0(V/s_a)^2/(2\sigma_d)=4 \times 10^{-7}$ and $E_d/\sigma_d=1000$. Diaphragm with large initial stress.

remaining factor of 1000 is due to the fact that the diaphragm with a large initial stress (membrane) needs a force per unit area that is about 1000 times larger than the same diaphragm without any initial stress (thin plate) for the same deflection. This effect is also illustrated by the difference in bias voltages, as mentioned in this Section, being 3.7 V for the membrane and 0.185 V for the thin plate.

4. Mechanical sensitivity of the condenser microphone

In the preceding Sections the static behaviour of a condenser microphone has been analysed. During normal operation, however, an a.c. signal is generated at the output terminals of the microphone due to a movement of the diaphragm, which is caused by an acoustic pressure on the diaphragm. The relation between the small-signal pressure on the diaphragm and the small-signal movement of the diaphragm is determined by the mechanical sensitivity, whereas the relation between the small-signal movement and the small-signal open-circuit output voltage is determined by the electrical sensitivity.

In this Section an analysis of the mechanical sensitivity will be given.

Equilibrium of the small-signal forces leads to

$$\frac{dw_0}{dP} = \frac{1}{\frac{d\bar{P}_r}{dw_0} - \frac{d\bar{P}_e}{dw_0}} \quad (26)$$

The mechanical sensitivity is defined as [16, 21]

$$S_m = \frac{dw_0}{dP} \quad (27)$$

where dw_0 can be considered as a change in the centre deflection of the diaphragm due to a change dP in the external pressure.

4.1 Mechanical sensitivity of the microphone with a stress-free diaphragm

Equation (27) can be rewritten for thin plates (stress-free diaphragms) by using eqns (14) and (26), resulting in

$$S_m = \frac{1}{3 \left(\frac{d\bar{P}_r}{dw_0} - \frac{d\bar{P}_e}{dw_0} \right)} \quad (28)$$

The first part of the denominator can be calculated by differentiating eqn (13) with respect to w_0

$$\frac{d\bar{P}_r}{dw_0} = \frac{1}{3} \frac{E_d}{0.171 R^4} \left(\frac{1}{h} + 1.464 \frac{w_0^2}{h^3} \right) \quad (29)$$

The second part of the denominator of eqn (28) can be described as

$$\frac{d\bar{P}_e}{dw_0} = \frac{\partial \bar{P}_e}{\partial w_0} + \frac{\partial \bar{P}_e}{\partial V} \frac{dV}{dw_0} \quad (30)$$

because \bar{P}_e is a function of both w_0 and V , while V is a function of w_0 only.

For the calculation of dV/dw_0 , an amplifier is considered to be used with an input capacitance C_i . During operation the total charge on both the microphone capacitance C_m , which is a function of w_0 [20], and the input capacitance C_i , is constant. Consequently, dV/dw_0 can be calculated, whereas with eqn (15) both $\partial \bar{P}_e/\partial w_0$ and $\partial \bar{P}_e/\partial V$ can be calculated. With these results, the value of $d\bar{P}_e/dw_0$ can now be calculated [20]

$$\begin{aligned} \frac{d\bar{P}_e}{dw_0} = & \frac{\epsilon_0 V^2}{2w_0^2} \left\{ - \frac{3s_a - 5w_0}{4(s_a - w_0)^2} \right. \\ & + \frac{3}{8(s_a w_0)^{1/2}} \ln \left[\frac{s_a^{1/2} + w_0^{1/2}}{s_a^{1/2} - w_0^{1/2}} \right] \\ & - \frac{\frac{1}{2} \pi \epsilon_0 R^2}{C_i + \frac{\pi \epsilon_0 R^2}{2(s_a w_0)^{1/2}} \ln \left[\frac{s_a^{1/2} + w_0^{1/2}}{s_a^{1/2} - w_0^{1/2}} \right]} \\ & \left. \times \left[\frac{1}{s_a - w_0} - \frac{1}{2(s_a w_0)^{1/2}} \ln \left(\frac{s_a^{1/2} + w_0^{1/2}}{s_a^{1/2} - w_0^{1/2}} \right) \right]^2 \right\} \quad (31) \end{aligned}$$

where V^2 can be eliminated by substitution of the right-hand part of eqn (18).

The mechanical sensitivity can now be calculated by substituting eqns (29) and (31) in eqn (28). The expression for the mechanical sensitivity will, however, not be shown in this Section, because of its complexity.

By dividing the mechanical sensitivity, dw_0/dP , by s_a/E_d , the expression for the sensitivity changes into a dimensionless shape

$$S_{mn} = \frac{d \left(\frac{w_0}{s_a} \right)}{d \left(\frac{P}{E_d} \right)} = \frac{\frac{1}{3}}{\left(\frac{d\bar{P}_r}{dw_0} - \frac{d\bar{P}_e}{dw_0} \right) \frac{s_a}{E_d}} \quad (32)$$

where $d\bar{P}_r/dw_0$ and $d\bar{P}_e/dw_0$ have to be replaced by eqns (29) and (31), respectively.

In Fig. 5 the normalized mechanical sensitivity is shown as a function of w_0/s_a for different values of the input capacitance C_i , divided by s_a , with $R/s_a = 1000$ and $h/s_a = 1$. As can be seen from this Figure, the mechanical sensitivity increases with increasing static deflection w_0 . This phenomenon is caused by the strong electric field

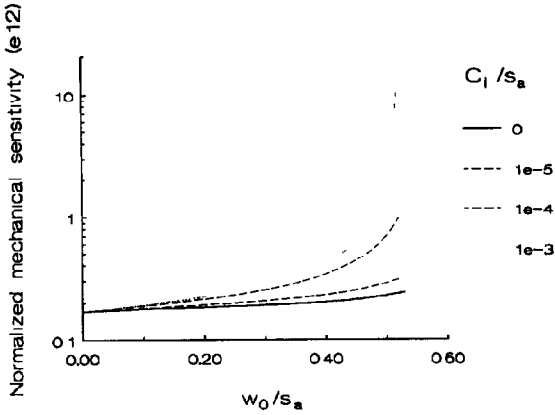


Fig 5 Normalized mechanical sensitivity as a function of the normalized centre deflection w_0/s_a for different values of C_1/s_a (F/m), with $h/s_a=1$ and $R/s_a=1000$ Diaphragm without initial stress

in the air gap of microphones, and, consequently, it is not found in other types of capacitive pressure sensors [22, 23]

It is also shown that increasing the input capacitance results in an increase in the mechanical sensitivity, especially at large deflections of the diaphragm. This phenomenon can be explained by considering two extreme circumstances where the diaphragm would have a piston-like movement. If an ideal voltage amplifier with $C_1=0$ is used, the charge on the plates of the microphone capacitance would be constant, although the diaphragm is moving. Consequently, the electric field in the air gap and the electrostatic force are constant. With $d\bar{P}_e/dw_0=0$, the mechanical sensitivity becomes equal to $(1/3)(d\bar{P}_r/dw_0)^{-1}$, resulting in a mechanical sensitivity that decreases with increasing static deflection according to eqn (29).

However, if an ideal charge amplifier is used and the voltage is constant, the electric field increases with increasing static deflection w_0 of the diaphragm, and, therefore, $d\bar{P}_e/dw_0 > 0$. Consequently, the mechanical sensitivity is much higher than when a voltage amplifier is used. At the largest possible static deflection, which has been described in Section 3.1, the value of $d\bar{P}_e/dw_0$ even becomes equal to $d\bar{P}_r/dw_0$, resulting in an infinitely high mechanical sensitivity.

Nevertheless, it will be shown in Section 7 that the use of a charge amplifier does not automatically result in the optimal overall performance of the microphone, although the total sensitivity is higher than when a voltage amplifier is used.

4.2 Mechanical sensitivity of the microphone with a diaphragm with a large initial stress

By using eqns (21) and (26), eqn (27) becomes, for diaphragms with a large initial stress,

$$S_m = \frac{1}{2 \left(\frac{d\bar{P}_r}{dw_0} - \frac{d\bar{P}_e}{dw_0} \right)} \quad (33)$$

As in Section 4.1, it can be derived for diaphragms with a large initial stress, which have a quadratic curvature according to eqn (5), that [20]

$$\frac{d\bar{P}_r}{dw_0} = 2 \frac{\sigma_d h}{R^2} + 4.785 E_d h \frac{w_0^2}{R^4} \quad (34)$$

and

$$\frac{d\bar{P}_e}{dw_0} = \frac{\epsilon_0 V^2}{2w_0^2} \left\{ \frac{2}{w_0} \ln \left(\frac{s_a}{s_a - w_0} \right) + \frac{-2s_a + 3w_0}{(s_a - w_0)^2} \right. \\ \left. - \frac{\left[\frac{1}{s_a - w_0} + \frac{1}{w_0} \ln \left(1 - \frac{w_0}{s_a} \right) \right]^2}{C_1 + \frac{\pi \epsilon_0 R^2}{w_0} \ln \left(\frac{s_a}{s_a - w_0} \right)} \right\} \quad (35)$$

where V^2 has to be replaced by the right-hand part of eqn (25).

The mechanical sensitivity can be calculated by using eqn (33) with the substitution of eqns (34) and (35). Again, the expression for the mechanical sensitivity is not shown in this Section because of its complexity.

By dividing the mechanical sensitivity by s_a/σ_d , the expression for the sensitivity changes into a dimensionless shape

$$S_{mn} = \frac{d \left(\frac{w_0}{s_a} \right)}{d \left(\frac{P}{\sigma_d} \right)} = \frac{1}{2 \left(\frac{d\bar{P}_r}{dw_0} - \frac{d\bar{P}_e}{dw_0} \right) \frac{s_a}{\sigma_d}} \quad (36)$$

where $d\bar{P}_r/dw_0$ and $d\bar{P}_e/dw_0$ have to be substituted by eqns (34) and (35), respectively.

In Fig 6 this normalized mechanical sensitivity is shown as a function of w_0/s_a for different values of the input capacitance C_1 , divided by s_a , with $R/s_a=1000$, $h/s_a=1$ and $E_d/\sigma_d=1000$. The curves have the same shape as in Fig. 5.

A comparison of Fig 6 with Fig 5 leads to a similar discussion to that mentioned at the end of Section 3.2: the mechanical sensitivity of microphones with a diaphragm with a large initial stress (membrane) is about 1000 times smaller than the sensitivity of the same microphones with a stress-free diaphragm (thin plate).

Nevertheless, the larger mechanical sensitivity of thin plates does not imply that the overall performance of microphones with a thin plate is much better than the

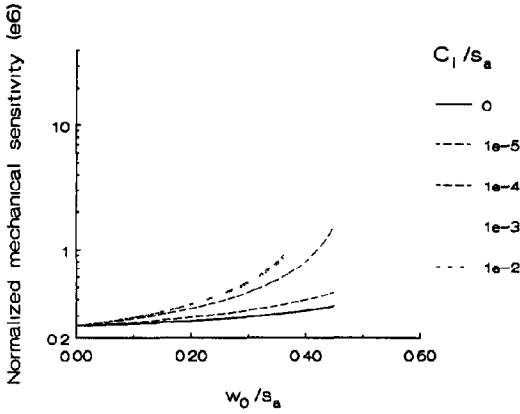


Fig 6 Normalized mechanical sensitivity as a function of the normalized centre deflection w_0/s_a for different values of C_i/s_a (F/m), with $h/s_a=1$, $R/s_a=1000$ and $E_d/\sigma_d=1000$ Diaphragm with large initial stress

performance of microphones with a membrane, as will be shown in Sections 6 and 7

5. Electrical sensitivity of the condenser microphone

The open-circuit electrical sensitivity is defined as [16, 21]

$$S_c = \frac{dV}{dw_0} \tag{37}$$

where dV can be considered as a change in the voltage due to a change in the centre deflection of the diaphragm dw_0 . Note that S_c has already been calculated in the previous Section by taking $C_i=0$

5.1 Electrical sensitivity of the microphone with a stress-free diaphragm

For stress-free diaphragms the electrical sensitivity becomes

$$S_c = -\frac{V}{s_a - w_0} \left[\frac{(s_a/w_0)^{1/2}}{\ln\left(\frac{s_a^{1/2} + w_0^{1/2}}{s_a^{1/2} - w_0^{1/2}}\right)} - \frac{s_a - w_0}{2w_0} \right] \tag{38}$$

The normalized, dimensionless electrical sensitivity S_{en} can be obtained by dividing eqn (38) by V/s_a

$$S_{en} = \frac{1}{V} \frac{dV}{d(w_0/s_a)} = -\frac{1}{1 - \frac{w_0}{s_a}} \left[\frac{(s_a/w_0)^{1/2}}{\ln\left(\frac{s_a^{1/2} + w_0^{1/2}}{s_a^{1/2} - w_0^{1/2}}\right)} - \frac{s_a - w_0}{2w_0} \right] \tag{39}$$

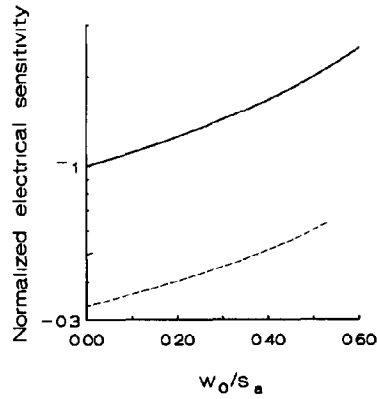


Fig 7 Normalized electrical open-circuit sensitivity as a function of the normalized centre deflection w_0/s_a , for a diaphragm without initial stress (thin plate, ---), a diaphragm with a large initial stress (membrane,) and a piston-like diaphragm (piston, —)

In Fig 7 this normalized electrical sensitivity is shown as a function of w_0/s_a (thin plate). As can be seen from this Figure, the electrical sensitivity is negative: an increase in the deflection w_0 causes a decrease in the voltage. It is obvious that the magnitude of the normalized electrical sensitivity increases with increasing static deflection, because the electric field increases with increasing static deflection.

Note that the magnitude of the normalized electrical sensitivity is equal to $1/3$ for very small values of w_0/s_a , which is due to the fourth-order polynomial curvature of the deflection.

5.2 Electrical sensitivity of the microphone with a diaphragm with a large initial stress

For diaphragms with a large initial stress the electrical sensitivity becomes

$$S_c = -\frac{V}{s_a - w_0} \left[\frac{1}{\ln\left(\frac{s_a}{s_a - w_0}\right)} - \frac{s_a - w_0}{w_0} \right] \tag{40}$$

The normalized, dimensionless, electrical sensitivity S_{en} is

$$S_{en} = \frac{1}{V} \frac{dV}{d(w_0/s_a)} = -\frac{1}{1 - \frac{w_0}{s_a}} \left[\frac{1}{\ln\left(\frac{s_a}{s_a - w_0}\right)} - \frac{s_a - w_0}{w_0} \right] \tag{41}$$

In Fig 7 this normalized electrical sensitivity is shown as a function of w_0/s_a (membrane)

The magnitude of the electrical sensitivity is always larger than in the case of a thin plate (no stress) and becomes equal to 1/2 for very small values of w_0/s_a . The value of 1/2 is caused by the parabolic curvature of the deflection

Note that in the case of a piston-like diaphragm, the electrical sensitivity dV/dw_0 is equal to $-V/(s_a - w_0)$, and, consequently, the normalized sensitivity is equal to $-1/(1 - w_0/s_a)$, which is also shown in Fig 7 (piston). In this case, the magnitude of the electrical sensitivity becomes equal to 1 for small values of w_0/s_a .

6. Total open-circuit sensitivity of the condenser microphone

The total open-circuit sensitivity of the condenser microphone is obtained by multiplying the mechanical sensitivity by the electrical sensitivity ($S_{tot} = S_m S_e$). Because the electrical sensitivity is negative and the mechanical sensitivity is positive, the total sensitivity will be negative. However, in the remaining part of this paper, only the magnitude of the total sensitivity will be considered. Therefore, in the next Sections the term total sensitivity denotes the absolute value of the sensitivity

6.1 Total sensitivity of the microphone with a stress-free diaphragm

The total sensitivity of a microphone with a diaphragm without initial stress can be calculated by multiplying the right-hand part of eqn (38) with the right-hand part of eqn (28), with substitution of eqns (29) and (31) in eqn (28). The expression for the total sensitivity is not shown here because of its complexity.

In Fig 8(a) this total sensitivity of the microphone is shown as a function of w_0/s_a for four values of E_d/s_a^2 , for $R/s_a = 1000$, $h/s_a = 1$ and $C_i = 0$. The dependence of the total sensitivity on R/s_a and h/s_a is shown in Fig 8(b), with $w_0/s_a = 0.25$ and $E_d/s_a^2 = 1 \times 10^{23}$ Pa/m².

In Fig 8(a) it is seen that the sensitivity increases with increasing static deflection and with decreasing E_d/s_a^2 . Figure 8(b) shows that the sensitivity increases with increasing value of R/s_a and decreasing h/s_a .

An analysis of the mechanical sensitivity, described by eqn (28) with eqns (29), (31) and (18), shows that for static deflections small compared with the diaphragm thickness h (large values of h/s_a) the mechanical sensitivity is proportional to $R^4/(E_d h^3)$. In eqns (38) and (18) it is shown that the electrical sensitivity is proportional to $(E_d h^3)^{1/2}/R^2$. Consequently, the total sensitivity is proportional to $R^2/(E_d h^3)^{1/2}$ as can be seen in Fig 8(a) and (b) (for large values of h/s_a).

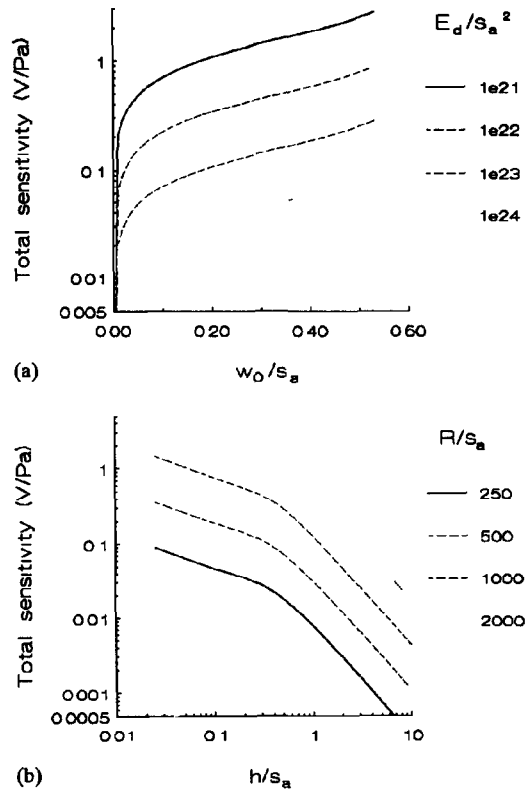


Fig 8 (a) Total open-circuit sensitivity as a function of the normalized centre deflection w_0/s_a for different values of E_d/s_a^2 (Pa/m²), with $h/s_a = 1$, $R/s_a = 1000$ and $C_i = 0$, (b) total sensitivity as a function of h/s_a for different values of R/s_a , with $w_0/s_a = 0.25$, $E_d/s_a^2 = 1 \times 10^{23}$ Pa/m² and $C_i = 0$. Diaphragm without initial stress

For relatively large deflections, where $w_0/h \gg 1.4$, the mechanical sensitivity is proportional to $R^4/(E_d h)$, according to eqns (28), (29), (31) and (18), and the electrical sensitivity is proportional to $(E_d h)^{1/2}/R^2$, according to eqns (38) and (18). Consequently, the total sensitivity is proportional to $R^2/(E_d h)^{1/2}$. This is illustrated in Fig 8(b) (for small values of h/s_a).

From these results, it can be concluded that maximum sensitivity is obtained at large static deflections, for small values of E_d and h , and for large values of R . One should keep in mind that the mechanical sensitivity is a function of the amplifier input capacitance C_i , and increases with increasing C_i , as shown in Section 4.1. If a charge amplifier is used, having an infinite value of C_i , the total sensitivity becomes infinitely high for the maximum allowed static deflection. However, the shape of the curves in Fig 8(a) and (b) does not change dramatically with changing values of C_i .

6.2 Total sensitivity of the microphone with a diaphragm with a large initial stress

The total sensitivity of the microphone with a diaphragm with a large initial stress can be obtained by

multiplying the electrical sensitivity, written in eqn (40), with the mechanical sensitivity, described by eqn (33) with substitution of eqns (34) and (35). Again, the expression for the total sensitivity is not shown here because of its complexity.

The total sensitivity of the microphone is shown in Fig 9(a) as a function of w_0/s_a for four values of σ_d/s_a^2 , and in Fig 9(b) as a function of h/s_a for four values of R/s_a .

From Fig 9(a) it can be seen that the total sensitivity increases with increasing static deflection of the diaphragm and decreasing σ_d/s_a^2 . In Fig 9(b) it is shown that the total sensitivity increases with decreasing h/s_a and increasing R/s_a .

Again, these results can be explained by analysing the expressions for the mechanical and the electrical sensitivity. Equations (33), (34), (35) and (25) show that the mechanical sensitivity is proportional to $R^2/(\sigma_d h)$, whereas eqns (40) and (25) show that the electrical sensitivity is proportional to $(\sigma_d h)^{1/2}/R$. Con-

sequently, the total sensitivity is proportional to $R/(\sigma_d h)^{1/2}$, which can be seen in Fig 9.

From these considerations, it can be concluded that maximum sensitivity is obtained at large static deflections, for small values of σ_d and h , and for large values of R . The Young's modulus is of negligible influence. Keep in mind that the mechanical sensitivity and, consequently, the total open-circuit sensitivity, will increase with increasing amplifier input capacitance C_i , which is not shown in Fig 9(a) and (b).

7. Overload of the microphone

If the sensitivity of the microphone is very high, the diaphragm might collapse into the direction of the backplate due to a relatively high (sound) pressure, which should be prevented. Therefore, it is important to calculate the maximum allowable pressure before the diaphragm collapses.

An external load, such as a sound pressure, causes an increase in the deflection of the diaphragm, resulting in an increase in the effective value of the electrostatic attractive force per unit area, \tilde{P}_e , and the reaction force per unit area, \tilde{P}_r . The effect of this phenomenon can be demonstrated with Fig 3 for microphones with a thin plate (stress-free diaphragm). For the situation shown in this Figure, the normalized static deflection w_0/s_a is equal to 0.23, which is the stable working point as described in Section 3.1. Due to a sound pressure, w_0/s_a increases, and the value of the sound pressure can be derived from the distance between the curve $(\tilde{P}_e - \tilde{P}_r)/E_d$ (dotted curve) and the x -axis in Fig 3. At a normalized deflection w_0/s_a equal to 0.63, the maximum allowable sound pressure occurs. For larger values of the sound pressure, the sum of this pressure and the electrostatic attractive force per unit area \tilde{P}_e is larger than the reaction force per unit area \tilde{P}_r , and the diaphragm collapses. Therefore, the normalized maximum allowable sound pressure \tilde{P}/E_d will be equal to 0.04×10^{-11} if the normalized static deflection w_0/s_a is equal to 0.23, as shown in Fig 3. Because the effective values of the forces per unit area are shown in Fig 3, the maximum allowable sound pressure has to be multiplied by a factor of three, according to eqn (14), resulting in a maximum normalized pressure P_{max}/E_d of 0.12×10^{-11} . This calculation can be carried out for every normalized static deflection w_0/s_a , resulting in a relation between the maximum normalized pressure P_{max}/E_d and the normalized static deflection w_0/s_a .

Note that this consideration is only valid when the voltage is kept constant, which is the case if a charge amplifier is used. If a voltage amplifier is used with an input capacitance C_i , the voltage between the two plates of the microphone capacitor will decrease with

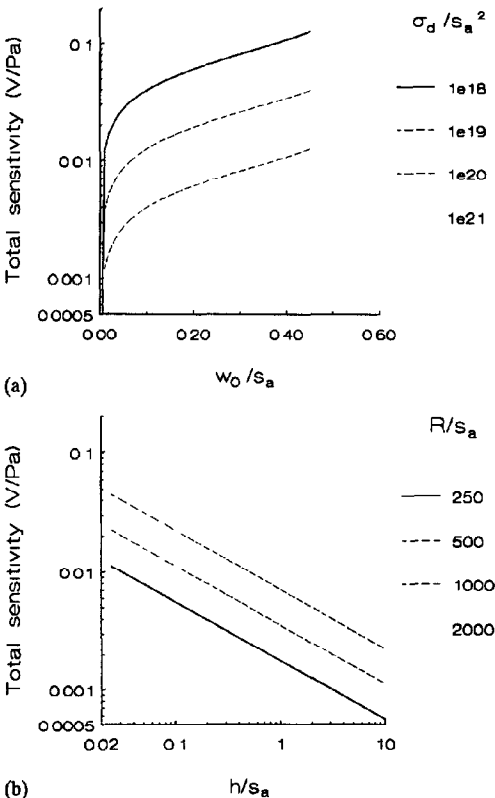


Fig 9 (a) Total open-circuit sensitivity as a function of the normalized centre deflection w_0/s_a for different values of σ_d/s_a^2 (Pa/m^2), with $h/s_a=1$, $R/s_a=1000$, $E_d/\sigma_d=1000$ and $C_i=0$, (b) total sensitivity as a function of h/s_a for different values of R/s_a , with $w_0/s_a=0.25$, $\sigma_d/s_a^2=1 \times 10^{20} \text{ Pa}/\text{m}^2$, $E_d/\sigma_d=1000$ and $C_i=0$. Diaphragm with large initial stress

increasing deflection due to a sound pressure. Therefore, the electrostatic force per unit area will increase less rapidly with increasing deflection than described in the previous paragraph. It is obvious that in this case the maximum allowable sound pressure will be larger than when the voltage is kept constant.

In Fig. 10 the maximum allowable pressure is shown as a function of the normalized static deflection w_0/s_a for different values of the normalized input capacitance C_i/s_a for microphones with a thin plate.

For microphones with a membrane a similar consideration can be applied, and the normalized maximum allowable pressure P_{\max}/σ_d is shown as a function of the normalized static deflection w_0/s_a in Fig. 11. Again, it can be seen that the maximum allowable sound pressure decreases with increasing static deflection of the membrane.

As can be seen from these Figures, an increase in the deflection and, consequently, in the sensitivity,

introduces a reduction of the maximum allowable sound pressure.

Therefore, a simple maximization of the microphone sensitivity does not result in an optimally designed microphone, because stability problems of very sensitive microphones can be expected if the sound pressure becomes too high.

8. Experimental

The verification of all the considerations described in the previous Sections would require many measurements, and would result in a lengthy description and discussion of the measurements, assuming that they are possible. Therefore, only two measurement results will be presented here, being the verification of Figs. 6 and 9(a), describing the dependence of the mechanical sensitivity on the static diaphragm deflection and the input capacitance of the preamplifier, and the total microphone sensitivity of the microphone as a function of the static deflection. Because the static deflection itself cannot be directly measured, the voltage that caused this static deflection will be calculated by using eqn. (25). Only microphones with a diaphragm having a large initial stress will be considered.

8.1 Measurement of the mechanical sensitivity

By using an optical measurement set-up [24], which can measure the curvature of reflecting diaphragms, the dependence of the mechanical sensitivity on the bias voltage has been measured. The output potential of the optical measurement system is a qualitative measure, which is linearly related to the diaphragm deflection.

The device used for this experiment was a square silicon condenser microphone with a $2\ \mu\text{m}$ thick Mylar diaphragm and an air-gap thickness of $40\ \mu\text{m}$, which has been described by Sprenkels [16]. The diaphragm area of the microphone was $6\ \text{mm}^2$ and the initial stress of the Mylar foil was approximately $2 \times 10^7\ \text{Pa}$.

In Fig. 12 the same calculated curves as shown in Fig. 6 are shown as a function of the bias voltage instead of the deflection by using eqn. (25). Because only the shape of the curves is considered, the mechanical sensitivity has been calculated for the same parameter values as used for Fig. 6, with $s_a = 40\ \mu\text{m}$.

In Fig. 13 the output voltage of the optical measurement system is shown as a function of the bias voltage for two different values of the input capacitance. The upper curve is measured by connecting the voltage source directly between the backplate contact and the diaphragm-electrode contact. In this way, the voltage is kept constant and the situation of an infinitely large amplifier input capacitance C_i has been simulated. The other curve is obtained by using a $7\ \text{G}\Omega$ resistor in

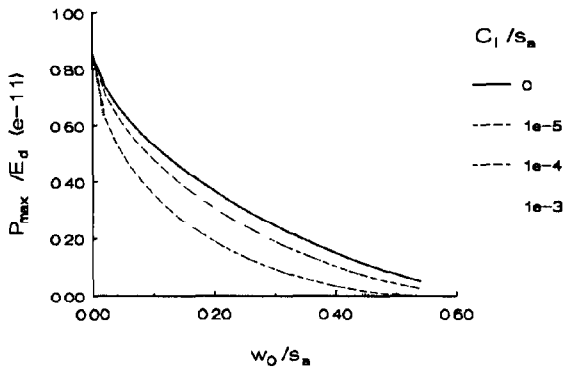


Fig. 10 Normalized maximum allowable acoustic pressure P_{\max}/E_d as a function of the normalized centre deflection w_0/s_a for different values of C_i/s_a (F/m), with $h/s_a=1$, $R/s_a=1000$ and $E_d/s_a^2=1 \times 10^{23}$. Diaphragm without initial stress.

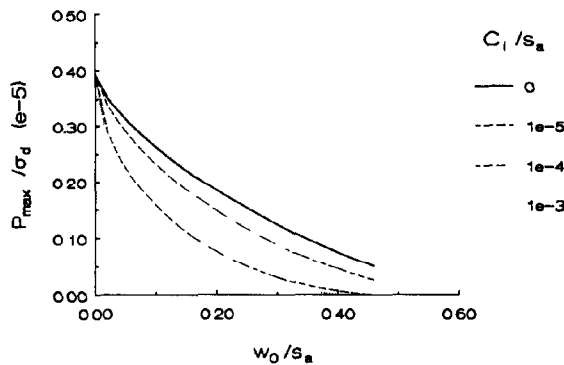


Fig. 11 Normalized maximum allowable acoustic pressure P_{\max}/σ_d as a function of the normalized centre deflection w_0/s_a for different values of C_i/s_a (F/m), with $h/s_a=1$, $R/s_a=1000$, $E_d/s_a^2=1000$ and $\sigma_d/s_a^2=1 \times 10^{20}$. Diaphragm with large initial stress.

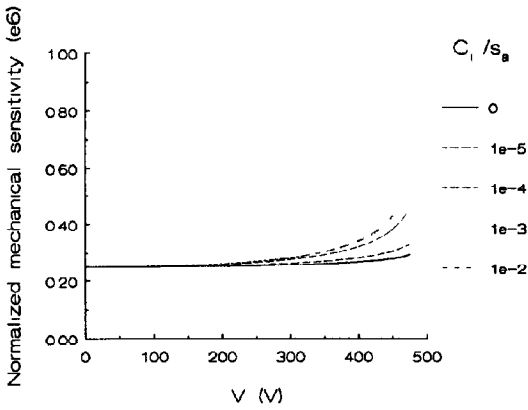


Fig 12 Normalized mechanical sensitivity as a function of the bias voltage V for different values of C_1/s_a (F/m), with $h/s_a=1$, $R/s_a=1000$ and $E_d/\sigma_d=1000$. Diaphragm with large initial stress

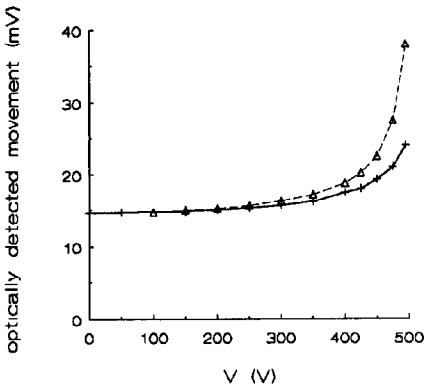


Fig 13 Optically detected mechanical sensitivity as a function of the bias voltage if the charge is kept constant (lower curve, $+ - +$) and if the voltage is kept constant (upper curve, $- \Delta -$)

series with the voltage source, resulting in a situation where the microphone charge is kept constant if the resistor has a zero shunt capacitance

Because the diaphragm movement at a constant sound pressure is proportional to the mechanical sensitivity, the vertical axes of Figs 12 and 13 can be compared. The comparison shows that the experimental results are in good agreement with the theoretically expected results. The lower curve in Fig 13 increases more rapidly than the zero-capacitance curve in Fig 12 because of the parasitic capacitance that was present during the measurements. The measurement has been carried out for two devices, which did not show any significant difference in measurement results

8.2 Measurement of the total sensitivity

The total sensitivity has been measured for two microphone types. The first type is the one used in the previous Section. During the experiments a JFET

source-follower was used. In Fig 14 the theoretically expected sensitivity (solid curve), as described in Section 6.2, is shown as a function of the bias voltage V for a microphone with a radius R of 1.4 mm (having the same diaphragm area as the microphone described in the previous Section), an air gap s_{a0} of 40 μm , a Young's modulus E_d of the Mylar diaphragm of 4×10^9 Pa, an initial stress σ_d of 2×10^7 Pa and a diaphragm thickness h of 2 μm . The amplifier input capacitance was taken equal to 2 pF, and the capacitive attenuation due to the presence of this capacitance was taken into account. The experimental results are also shown in the Figure (denoted by crosses)

The second type is a microphone presented by Scheeper *et al* [25], having a square silicon nitride diaphragm with an initial stress of 1.5×10^8 Pa, and a silicon nitride backplate with an initial stress of 3×10^7 Pa. The air-gap thickness s_{a0} is 3.6 μm , the surface area 15×15 mm^2 , and the thickness of the diaphragm and the backplate are both 1 μm .

In Fig 15 the theoretically expected sensitivity (solid curve), according to the description in Section 6.2, is shown for a circular microphone with a radius of 0.84 mm (having the same diaphragm area as the square microphone with an area of 15×15 mm^2) and an amplifier input capacitance C_1 of 5 pF. Note that this capacitance is taken to be extra large because of the relatively large parasitic capacitance of this device. The calculated static deflection of this device, which can be calculated with eqn (25), had to be adjusted, because the relatively thin backplate also had a static deflection. In the same Figure the experimental results are shown for this device, denoted by crosses.

For both types of microphones, the measured sensitivities are in reasonable agreement with the theoretically expected values. Therefore, it can be concluded that the models for condenser microphones, described

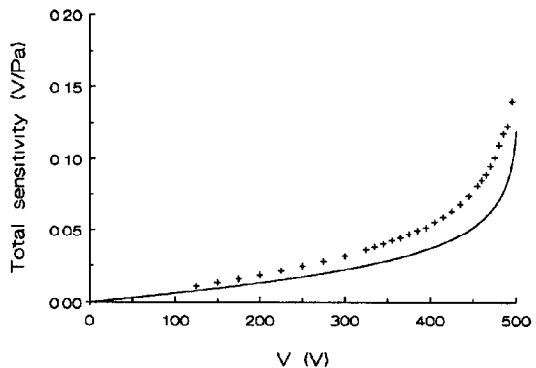


Fig 14 Total sensitivity of a microphone with a Mylar diaphragm, calculated with $s_a=40$ μm , $h=2$ μm , $R=1.4$ mm, $\sigma_d=2 \times 10^7$ Pa, $E_d=4 \times 10^9$ Pa, and $C_1=2$ pF (solid curve), and measured sensitivity (denoted by crosses)

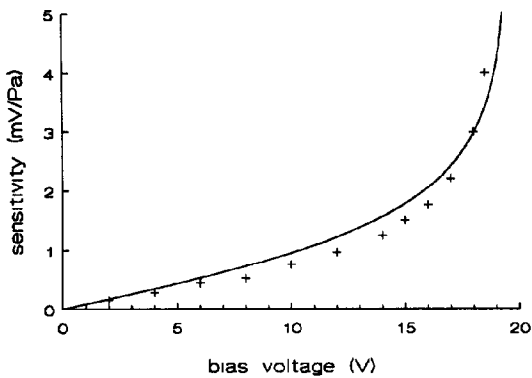


Fig 15 Total sensitivity of a microphone with a silicon-nitride diaphragm, calculated with $s_{a0} = 3.4 \mu\text{m}$, $h = 1 \mu\text{m}$, $R = 0.85 \text{ mm}$, $\sigma_d = 1.5 \times 10^8 \text{ Pa}$, $E_d = 1.5 \times 10^{11} \text{ Pa}$, and $C_i = 5 \text{ pF}$ (solid curve), and measured sensitivity (denoted by crosses)

in this paper, are a useful tool for predicting the behaviour of condenser microphones. The difference between square (reality) and circular (model) diaphragms is obviously of minor importance.

9. Discussion and conclusions

In this paper a theoretical analysis has been given concerning condenser microphones with a circular diaphragm without initial stress and with a large initial stress.

It is shown that the mechanical sensitivity increases with increasing static centre deflection of the diaphragm and with increasing input capacitance of the preamplifier. The sensitivity can theoretically even become infinitely high at large static deflections if a charge amplifier is used.

The electrical open-circuit sensitivity increases with increasing static centre deflection.

Consequently, the maximum possible total sensitivity can be obtained by taking the highest possible bias voltage V , resulting in a maximum deflection of the diaphragm. If the value of the input capacitance of the amplifier is infinite, which occurs if a charge amplifier is used, the value of the sensitivity theoretically also becomes infinite. However, in this situation a small sound pressure might already cause a collapse of the diaphragm. Therefore, the maximum microphone sensitivity and the maximum deflection are limited by a maximum allowable sound pressure that has to be specified. Higher pressures will cause a collapse of the diaphragm.

If both this maximum allowable sound pressure and the considerations concerning noise performance of condenser microphones with a preamplifier [26, 27] are taken into account, it is possible to optimize the overall

performance of a condenser microphone with a preamplifier.

Experiments carried out to analyse the mechanical sensitivity and the total sensitivity show a good agreement between the model of microphones with a highly tensioned diaphragm and the measurement results.

References

- 1 J E Warren, A M Brzezinski and J F Hamilton, Capacitance-microphone static membrane deflections, *J Acoust Soc Am*, 52 (1972) 711-719
- 2 J E Warren, Capacitance-microphone static membrane deflections comments and further results, *J Acoust Soc Am*, 58 (1975) 733-740
- 3 J E Warren, A M Brzezinski and J F Hamilton, Capacitance microphone dynamic membrane deflections, *J Acoust Soc Am*, 54 (1973) 1201-1213
- 4 S K Clark and K D Wise, Pressure sensitivity in anisotropically etched thin-diaphragm pressure sensors, *IEEE Trans Electron Devices*, ED-26 (1979) 1887-1896
- 5 H Ko, M-H Bao and Y-D Hong, A high-sensitive integrated circuit capacitive pressure transducer, *IEEE Trans Electron Devices*, ED-29 (1982) 48-56
- 6 H-L Chau and K D Wise, Scaling limits in batch-fabricated silicon pressure sensors, *IEEE Trans Electron Devices*, ED-34 (1987) 850-858
- 7 G Blasquez, Y Naciri, P Blondel, N Ben Moussa and P Pons, Static response of miniature capacitive pressure sensors with square or rectangular silicon diaphragm, *Rev Phys Appl*, 22 (1987) 505-510
- 8 D Hohm, *Kapazitive Silizium-Sensoren für Horschallanwendungen*, Fortschritt-berichte VDI, Reihe 10, Nr 60, Dusseldorf, 1986
- 9 J A Voorthuyzen and P Bergveld, The influence of tensile forces on the deflection of circular diaphragms in pressure sensors, *Sensors and Actuators*, 6 (1984) 201-213
- 10 J A Voorthuyzen, A J Sprenkels, A G H van der Donk, P R Scheeper and P Bergveld, Optimization of capacitive microphone and pressure sensor performance by capacitor-electrode shaping, *Sensors and Actuators A*, 25-27 (1991) 331-336
- 11 W Kühnel and G Hess, Micromachined subminiature condenser microphones in silicon, *Sensors and Actuators A*, 32 (1992) 560-564
- 12 P Murphy, K Hubschi, N de Rooij and C Racine, Subminiature silicon integrated electret capacitor microphone, *IEEE Trans Electron Instrum*, EI-24 (1989) 495-498
- 13 J Bergqvist and F Rudolf, A new condenser microphone in silicon, *Sensors and Actuators*, A21-A23 (1990) 123-125
- 14 J Bergqvist, F Rudolf, J Maisano, F Parodi and M Rossi, A silicon condenser microphone with a highly perforated backplate, *Proc 6th Int Conf Solid-State Sensors and Actuators (Transducers '91)*, San Francisco, CA, USA, June 24-28, 1991, pp 266-269
- 15 P R Scheeper, W Olthuis and P Bergveld, A silicon condenser microphone with a silicon nitride diaphragm and backplate, *J Micromech Microeng*, 2 (1992) 187-189
- 16 A J Sprenkels, A silicon subminiature electret microphone, Thesis, Twente University, 1988
- 17 E Frederiksen, N Eirby and H Mathiasen, Prepolarized condenser microphones for measurement purposes, *Noise and Vibration Control Worldwide*, (March) (1980) 88-96

- 18 S Timoshenko and S Woinowski-Krieger, *Theory of Plates and Shells*, McGraw-Hill, New York, 2nd edn, 1959
- 19 P R Scheeper, W Olthuis and P Bergveld, Fabrication of a subminiature silicon condenser microphone using the sacrificial layer technique, *Proc 6th Int Conf Solid-State Sensors and Actuators (Transducers '91)*, San Francisco, CA, USA, June 24-28, 1991, pp 408-411
- 20 A G H van der Donk, A silicon condenser microphone modelling and electronic circuitry, *Thesis*, Twente University, 1992
- 21 F Fram and P Murphy, Miniature electret microphones, *J Audio Eng Soc*, 18 (1970) 511-517
- 22 W H Ko, Solid-state capacitive pressure transducers, *Sensors and Actuators*, 10 (1986) 303-320
- 23 J A Voorthuyzen, P Bergveld and A J Sprengels, Semiconductor-based electret sensors for sound and pressure, *IEEE Trans Electrical Insul*, 24 (1989) 267-276
- 24 C M Lawson and V J Tekippe, Fiber-optic diaphragm-curvature pressure transducer, *Opt Lett*, 8 (1983) 286-288
- 25 P R Scheeper, W Olthuis and P Bergveld, A silicon condenser microphone with a silicon nitride diaphragm and backplate, *Proc Micromechanics Europe 1992 (MME '92)*, Leuven, Belgium pp 110-113
- 26 A G H van der Donk, J A Voorthuyzen and P Bergveld, Optimal design of electret microphone MOSFET preamplifier, *J Acoust Soc Am.*, 91 (1992) 2261-2269
- 27 A G H van der Donk, J A Voorthuyzen and P Bergveld, General considerations of noise in microphone preamplifiers, *Sensors and Actuators A*, 25-27 (1991) 515-520

Biographies

Armand Gysbertus Hennie van der Donk was born in Nijmegen, The Netherlands, on January 5, 1962. He received the M S degree in electrical engineering from the University of Eindhoven, The Netherlands in 1987. In 1988 he joined the Bio-Information Group, Department of Electrical Engineering, University of Twente, Enschede, The Netherlands, where he received his Ph D degree in 1992. His research was focused on the development of electronic circuitry for a microphone based on silicon technology for use in hearing aids. Currently he is working as an automotive sensor design engineer at Texas Instruments Holland B V.

Patrick Richard Scheeper was born in Nieuw Vennepe, The Netherlands, on October 25, 1965. He received the B S degree in applied physics from the Rooms Katholieke Hogere Technische School Rijswijk, Rijswijk, The Netherlands, in 1988. In the same year he joined the Bio-Information Group, Department of Electrical Engineering, University of Twente, The Netherlands, where he received his Ph D degree in 1993. His research was focused on the development of a microphone based on silicon technology for use in hearing aids. Currently he is working as a micromachining engineer at Bruel & Kjaer.

Wouter Olthuis was born in Apeldoorn, The Netherlands, on October 23, 1960. He received the M S degree in electrical engineering from the University of Twente, Enschede, The Netherlands, in 1986. In the same year he joined the Biomedical Engineering Division of the Faculty of Electrical Engineering, University of Twente, Enschede, The Netherlands, where he received his Ph D degree in 1990. Currently, he is working as an assistant professor in the biosensor technology group of the University of Twente.

Piet Bergveld was born in Oosterwolde, The Netherlands, on January 26, 1940. He received the M S degree in electrical engineering from the University of Eindhoven, The Netherlands, in 1965 and the Ph D degree from the University of Twente, The Netherlands, in 1973. The subject of his dissertation was the development of ISFETs and related devices, and the actual invention of the ISFET, since then also investigated by many other international research groups of universities as well as industry.

Since 1965 he has been a member of the Biomedical Engineering Division of the Faculty of Electrical Engineering (University of Twente) and was in 1984 appointed as full professor in Biosensor Technology. He is one of the project leaders in the MESA Research Institute.

His research subjects still concern the further development of ISFETs and biosensors based on ISFET technology as well as silicon microphones, resulting up to now in more than 150 papers.